American Mineralogist, Volume 99, pages 109–116, 2014

Aluminum ion occupancy in the structure of synthetic saponites: Effect on crystallinity

HONGPING HE[1,*], TIAN LI[1,2], QI TAO[1], TIANHU CHEN[3], DAN ZHANG[1,2], JIANXI ZHU[1], PENG YUAN[1] AND RUNLIANG ZHU[1]

[1]Key Laboratory of Mineralogy and Metallogeny, Guangzhou Institute of Geochemistry, Chinese Academy of Sciences, Guangzhou 510640, China
[2]University of Chinese Academy of Sciences, Beijing 100049, China
[3]School of Natural Resources and Environment, Hefei University of Technology, Hefei 230009, China

ABSTRACT

Two series of saponites with fixed (Si+Al)/Mg and Si/Mg ratios, respectively, were synthesized by using hydrothermal methods. The obtained products were characterized by XRD, XRF, ^{27}Al, and ^{29}Si MAS NMR, SEM, and TEM. XRD patterns showed that well-ordered saponites were obtained in the initial Si/Al ratio range of 5.43–7.89. Beyond this Si/Al ratio range, poorly crystallized saponites were obtained with small crystallized particles, which can be seen from TEM images. When intercalating saponite with surfactant, the intercalated products displayed strong and well-ordered (00*l*) reflections, indicating that layered saponite has been successfully synthesized in the present study. ^{27}Al MAS NMR spectra demonstrated that well-crystallized synthetic saponites had a higher Al(IV)/Al(VI) ratio than the poorly crystallized samples, which is an important factor affecting the crystallinity of synthetic saponite. A one-to-one substitution (i.e., 1 $Al^{3+} \rightarrow 1\ Mg^{2+}$) actually occurred in the octahedral sheet and this substitution had a negative effect on the crystallinity of the synthetic saponites. After grafting the synthetic saponites with silane, the decreased intensity of the ^{29}Si NMR signal at –86 ppm and the increased intensity of Q^3 Si(0Al) and Q^3 Si(1Al) signals strongly suggested that the signal at ca. –86 ppm corresponded to Q^2 Si at the layer edges of saponite.

Keywords: Synthetic saponite, occupancy of aluminum ion, crystallinity, ^{27}Al and ^{29}Si MAS NMR, isomorphous substitution

INTRODUCTION

Saponite is a 2:1 type trioctahedral phyllosilicate of the smectite group of clay minerals. The saponite structure is composed of a central octahedral sheet with essentially a brucite $[Mg_3(OH)_6]$ structure, in which four out of six OH^- groups are replaced by oxygen atoms. These oxygen atoms are connected to two tetrahedral sheets consisting of Si^{4+} and O^{2-} situated on both sites of the central octahedral sheet. The ideal structural formula of saponite can be presented as $M_x^+[Mg_3][Si_{4-x}Al_x]O_{10}(OH)_2{\cdot}nH_2O$, where M is the exchangeable interlayer cation (Brigatti et al. 2006).

Natural saponites are usually formed from weathering of Mg-containing rocks. Due to the complexities of the chemical compositions of the mother rocks and physical-chemical conditions in the geological process of saponite formation, isomorphous substitution of Al^{3+} for Si^{4+} in the tetrahedral sheet and Mg^{2+} by metals with different valences (e.g., Al^{3+}, Fe^{3+}, Li^+, Mn^{2+}, Ni^{2+}, Zn^{2+}) in the octahedral sheet extensively occurred (Mackenzie 1957; Vicente Rodriguez et al. 1994). Generally, the isomorphous substitution of Al^{3+} for Si^{4+} in the tetrahedral sheet is dominant and saponite is negatively charged, in which the net negative charges are compensated by exchangeable interlayer cations.

Because of its high surface acidity and thermal stability, saponite has been widely used as a heterogeneous catalyst and catalyst support (Varma 2002; Casagrande et al. 2005; Vogels et al. 2005a) as well as a filler in the preparation of polymer nanocomposites (Giannelis et al. 1999; Alexandre and Dubois 2000; Zanetti et al. 2000). The surface properties (e.g., acidity, interlayer swelling) of clay minerals are also highly dependent on their chemical composition which, in turn, is strongly affected by the extent of isomorphous substitution in their layer structure (Moronta 2004).

For industrial applications, it is very important that the composition and properties of clay materials can be adjusted for different industries. But for a specific field, the composition and property are demanded to be homogeneous. The chemical composition and property of natural saponites can be extremely variable, which strongly depend on the chemical composition of the mother rock, the genesis process and the provenance (Utracki et al. 2007). This variability represents a strong limitation in their applications especially when surface properties have to be strictly controlled, such as in catalysis.

For this reason, different methods have been developed to prepare synthetic saponites with well-controlled chemical composition and property (Farmer et al. 1991, 1994; Kloprogge et al. 1993, 1994a, 1994b; Vogels et al. 1997, 2005b; Kawi and Yao 1999; Yao et al. 2005; Higashi et al. 2007; Bisio et al. 2008; Vicente et al. 2010; Xue and Pinnavaia 2010). For instance, Farmer et al. (1991, 1994) synthesized well-formed saponite in hydrazine-water mixtures and found that the presence of Fe^{2+} in a calcareous environment may promote the formation of saponite. Different NH_4^+ saponites with variable crystallinity, platelet dimensions, specific surface areas and cation exchange capacities were obtained by varying synthesis gel composition and crystallization temperature (Kloprogge et al. 1993). Bisio et al. (2008) reported that different H_2O/Si molar ratios of the gels

* E-mail: hehp@gig.ac.cn

0003-004X/14/0001–109$05.00/DOI: http://dx.doi.org/10.2138/am.2014.4543

strongly affected the surface properties of the saponite samples, including texture, adsorption property, thermal stability, and acidity of surface species. These studies paid attention mainly to the influences of experimental conditions on the crystallinity and properties of synthetic saponites (Zhang et al. 2010).

In addition to the effects of synthesis conditions (e.g., starting materials, temperature, pressure, aging time, microwave heating) (Kloprogge et al. 1999; Zhang et al. 2010), a noteworthy problem is the occupancy of the substituting ions (e.g., Al^{3+}) in synthetic saponites, which is the key factor controlling the structure and properties of synthetic saponites. Isomorphous substitution will lead to a distortion of tetrahedral and octahedral sheets and a further effect on the stacking order of saponite layers (Kloprogge et al. 1994a). On the other hand, different types of substitution can result in a significant effect on net charges of synthetic saponites and a further effect on cation exchange capacity (CEC). For example, a muscovite substitution in the octahedral sheet (Vogels et al. 2005b), $2Al^{3+}$ + 1 vacancy $\rightarrow$ $3Mg^{2+}$, has no effect on the total net charges of saponite, whereas a one-to-one (1 Al^{3+} $\rightarrow$ 1 Mg^{2+}) substitution will create a positive charge (Suquet et al. 1981). The latter compensates a negative charge created by the substitution of Si^{4+} by Al^{3+} in the tetrahedral sheet and decreases the total net charge of saponite.

In this respect, Kloprogge and co-workers have conducted a series of investigations during the last two decades, by using a combination of various characterization techniques (Kloprogge et al. 1993, 1994a, 1994b; Vogels et al. 1997, 2005b). Al ions could occupy both tetrahedral and octahedral sites and the Al(IV)/Al(VI) ratio increased with increasing synthesis temperature (Kloprogge et al. 1994a 1994b). A muscovite substitution ($2Al^{3+}$ + vacancy $\rightarrow$ $3Mg^{2+}$) was proposed for the substitution of Al^{3+} for Mg^{2+} in the octahedral sheet of synthetic saponites (Vogels et al. 2005b). This is very different from the model (1 Al^{3+} $\rightarrow$ 1 Mg^{2+}) suggested by Suquet et al. (1981). These findings are helpful for understanding the structure and property of synthetic saponites. Unfortunately, further investigation about the relationship between the occupancy of the substituting Al^{3+} and the structure/property of synthetic saponite has not been reported so far.

The main aim of this study is to investigate occupancy priority of Al ions between tetrahedral and octahedral sites and its effect on the structure and crystallinity of synthetic saponites. Hence, two series of saponites with fixed (Si+Al)/Mg and Si/Mg ratios, respectively, were synthesized by using hydrothermal methods as described by Kawi and Yao (1999). The obtained saponites were characterized by X-ray diffraction (XRD), X-ray fluorescence spectroscopy (XRF), ^{27}Al and ^{29}Si solid-state magic-angle-spinning nuclear magnetic resonance spectroscopy (MAS NMR), scanning electron microscopy (SEM), and transmission electron microscopy (TEM).

Experimental methods

Preparation methods

Synthesis of saponite. Synthetic saponite samples were prepared by modifying the literature method indicated by Kawi and Yao (1999). The ratios of Si, Al, and Mg in the starting materials and the products are shown in Table 1. A general synthesis procedure is as follows: A buffer solution was prepared by dissolving 18.00 g of NaOH and 32.80 g of $NaHCO_3$ in 250 mL of deionized water. Then, desired amounts of sodium metasilicate ($Na_2SiO_3 \cdot 9H_2O$) solution were added to the buffer solution under vigorous stirring. The obtained solution was noted as Solution A. Solution B was prepared by dissolving desired amounts of $AlCl_3 \cdot 6H_2O$ and 30.80 g of $MgCl_2 \cdot 6H_2O$ in 25 mL of deionized water. Then, Solution B was slowly added into Solution A with continuous stirring until a uniform gel was eventually obtained. After that, the gel was transferred to a polytetrafluoroethylene-lined autoclave and treated at 160 °C for 24 h.

To exclude the excess electrolytes in the resultant products, the obtained products were washed 8 times with deionized water, then dried at 80 °C and ground before characterizations. The series of synthetic saponites with fixed (Si+Al)/Mg (Series I) was prepared by adjusting the amounts of $AlCl_3 \cdot 6H_2O$ and $Na_2SiO_3 \cdot 9H_2O$, and the obtained products were denoted as SAP-I-X, in which X stands for Si/Al ratio in the starting material. By the same method, the synthetic saponites with fixed Si/Mg (Series II) were prepared by adjusting the added amounts of $AlCl_3 \cdot 6H_2O$. The obtained products were marked as SAP-II-X (X = Si/Al ratio in the starting material). The cationic exchange capacity (CEC) of the synthesized saponites was determined by the method reported in the literature (Hu et al. 2000; Bisio et al. 2008). The synthetic saponites (500 mg) were exchanged with 30 mL of a 0.05 M solution of $[Co(NH_3)_6]^{3+}$. After separation by centrifugation, the solution was

Table 1. The molar ratios of Si, Al, and Mg in the starting materials, CEC, and Al(IV)/Al(VI) ratios of the synthetic saponites

Samples	Si:Al:Mg	Nominal Si/Al[a]	Measured Si/Al[b]	CEC[c] (mmol/100 g)	Al(IV)/Al(VI)[d]	Al(IV)[e] (%)
			Series I			
SAP-I-1.80	2.57:1.43:3.00	1.80	1.8	108	3.9	25.1
SAP-I-2.13	2.72:1.28:3.00	2.13	2.2	118	5.0	22.6
SAP-I-2.33	2.80:1.20:3.00	2.33	2.3	104	5.6	22.2
SAP-I-4.50	3.27:0.73:3.00	4.50	4.5	133	13.6	15.4
SAP-I-5.43	3.38:0.63:3.00	5.43	5.6	133	25.6	13.7
SAP-I-7.89	3.55:0.45:3.00	7.89	7.9	120	16.7	10.2
SAP-I-12.30	3.70:0.30:3.00	12.30	12.4	117	8.9	6.8
SAP-I-14.50	3.74:0.26:3.00	14.50	13.6	116	6.1	6.0
SAP-I-39.00	3.90:0.10:3.00	39.00	33.9	113	4.0	2.2
			Series II			
SAP-II-1.80	2.72:1.53:3.00	1.80	1.9	113	5.2	24.8
SAP-II-2.13	2.72:1.28:3.00	2.13	2.3	114	6.3	22.6
SAP-II-2.33	2.72:1.17:3.00	2.33	3.3	135	8.8	19.1
SAP-II-4.50	2.72:0.60:3.00	4.50	4.8	140	8.1	15.4
SAP-II-5.43	2.72:0.50:3.00	5.43	7.5	125	25.3	10.8
SAP-II-7.89	2.72:0.35:3.00	7.89	10.8	116	10.4	7.7
SAP-II-12.30	2.72:0.22:3.00	12.30	15.3	116	5.1	6.1
SAP-II-14.50	2.72:0.19:3.00	14.50	14.2	103	5.4	5.3
SAP-II-39.00	2.72:0.07:3.00	39.00	43.7	115	2.5	1.8

[a] Nominal Si/Al ratio in the synthesis gel based on the chemical composition of the starting solutions for the synthesis.
[b] Si/Al ratio in the synthetic saponites determined by XRF measurement, which has measurement errors within 5%.
[c] Accuracy of the CEC measurement is within 5%.
[d] Determined by deconvolution of ^{27}Al MAS NMR spectra with uncertainty of ±3%.
[e] Calculated percentage of Al(IV)/[Al(IV)+Si] in tetrahedral sheet with uncertainty of ±5%.

analyzed by UV–Vis spectrophotometer (UV-7504). The decrease of absorbance at 474 nm, typical of the CT transition of $[Co(NH_3)_6]^{3+}$, is quantitatively related to the difference in concentration by means of a calibration with standard solutions.

Intercalating saponite with surfactant. Intercalation experiments were carried out with hexadecyltrimethylammonium bromide (HDTMAB) at a concentration to yield an amount equivalent to the CEC of the saponite as described in the literature (He et al. 2010). A desired amount of HDTMAB was dissolved in 30 mL of distilled water. Then, 1.00 g of synthetic saponite (e.g., SAP-I-2.33, SAP-I-5.43, and SAP-I-7.89) was added into the prepared solution containing HDTMAB. The mixtures were stirred at 60 °C for 6 h. All the products were washed with deionized water six times and dried at 80 °C. The intercalated products prepared from SAP-I-2.33, SAP-I-5.43, and SAP-I-7.89 were marked as SAP-I-2.33-1CEC, SAP-I-5.43-1CEC, and SAP-I-7.89-1CEC, respectively.

Grafting saponite with silane. The grafting reaction was carried out in a mixture of water/ethanol (25/75 by volume) as reported in the literature (He et al. 2005). 3.00 g of synthetic saponite (SAP-I-5.43, SAP-I-12.30, and SAP-I-39.00) and 7.05 mL of 3-aminopropyltriethoxysilane (APTES, with a purity of 99%, from Aldrich) were mixed by stirring in 60 mL of water/ethanol mixture at 80 °C for 24 h. The products were filtered, washed six times using the mixture of water/ethanol and dried at 80 °C. Then, the resultant product was grounded and placed in a sealed container for characterization. The grafting products prepared from SAP-I-5.43, SAP-I-12.30, and SAP-I-39.00 were denoted as SAP-I-5.43-APTES, SAP-I-12.30-APTES, and SAP-I-39.00-APTES, respectively.

Analytical techniques

X-ray diffraction (XRD). Randomly oriented powder X-ray diffraction patterns (XRD), to determine the basal spacing of the sample, were collected between 1° and 80° (2θ) at a scanning rate of 1° (2θ) min^{-1} on a Bruker D8 Advance diffractometer with Ni-filtered Cu$K\alpha$ radiation (λ = 0.154 nm, 40 kV, and 40 mA).

Transmission electron microscopy (TEM). TEM images were collected on a JEOL 2010 high-resolution transmission electron microscope operated at an accelerating voltage of 200 kV. Specimens were prepared by dispersing the sample in ethanol and ultrasonically treating for 5 min. A drop of the resultant suspension was placed on a holey carbon film supported by a copper grid, after which the ethanol was evaporated. Chemical analysis was executed using the attached energy-dispersive X-ray (EDX) analyzer to obtain the molar ratio of Si, Al, and Mg in the synthetic saponites.

Field-emission scanning-electron microscopy (FE-SEM). SEM images were recorded on a Sirion-200 field emission scanning electron microscope, using a tungsten filament as electron source. Samples were disaggregated by sonication in ethanol. A conductive coating of gold by low-pressure plasma was finally deposited to avoid the electronic charging on the insulating particles under the electron beam.

X-ray fluorescence spectroscopy (XRF). Elemental analysis was conducted on a Rigaku RIX 2000 X-ray fluorescence spectrometer (XRF). Saponite samples were ground using an agate mortar to 200 mesh. Loss-on-ignition was obtained by weight loss of the sample ignited in a furnace at 900 °C for 2 h and allowed to cool in a desiccator to minimize moisture absorption. About 500 mg calcined saponite sample and 4 g $Li_2B_4O_7$ were mixed homogeneously, and the mixture was digested in a Pt-Au alloy crucible at 1150 °C in a high-frequency furnace. The quenched bead was used for XRF measurements (Goto and Tatsumi 1994). The calibration line for Si/Al ratio used in quantification was produced by bivariate regression of the Si/Al data measured for 36 reference materials encompassing a wide range of silicate compositions, and analytical uncertainties were mostly between 1 and 5%.

Magic angle spinning nuclear magnetic resonance spectroscopy (MAS NMR). Both ^{27}Al MAS NMR and ^{29}Si cross-polarization (CP) MAS NMR measurements were carried out on a Bruker AVANCE III 400 WB spectrometer. The resonance frequency of ^{29}Si was 79.5 MHz. Samples were packed in a 7 mm ZrO_2 rotor and spun at the magic angle (54.7°), and the spin rate was 7 kHz. ^{29}Si CPMAS NMR spectra were recorded with a contact time of 4.5 ms and a recycle delay of 2 s, using tetramethylsilane (TMS) as an external reference. The corresponding resonance frequency of ^{27}Al was 104.3 MHz. Samples were packed in a 4 mm ZrO_2 rotor and spun at the magic angle (54.7°), and the spin rate was 15 kHz. Single pulse magic angle spinning spectra were acquired using a high power 0.5 μs pulse, corresponding to a tip angle of 18° and a recycle delay of 0.5 s. The ^{27}Al chemical shift was externally referenced to a 1.0 M aqueous solution of $Al(NO_3)_3$. Peak component analysis was undertaken using a Gauss–Lorentz cross-product function applied by the PEAKFIT software package. The minimum number of component bands was obtained with squared correlations ≥0.995.

Results and discussion

Crystallinity and morphology of the synthetic saponites

Table 1 shows the molar ratios of Si, Al, and Mg in the synthesis gels, CEC, and Al(IV)/Al(VI) ratios of the synthesized saponites. In the case of Series I, the added amount of Mg and the total amount of Si and Al were fixed [i.e., (Si+Al):Mg = 4:3] while the Si/Al ratio was different from each other. For Series II, the added Si and Mg amounts were fixed and that of Al was varied, keeping an identical Si/Al ratio to that of the corresponding one in Series I. That is to say, samples in Series II can be considered as a case in which the added Mg amount was changed while the Si/Al ratio was identical to the corresponding one in Series I. This is helpful for us to well understand the influence of the added amount of Mg on the occupancy of Al in the synthetic saponites. As shown in Table 1, the nominal Si/Al ratios are similar to those measured, implying that the synthesis reaction is almost complete.

The powder XRD patterns of the synthetic saponites are shown in Figure 1. A series of reflections are recorded at ca. 1.33–1.41, 0.45–0.46, 0.26, and 0.153 nm, corresponding to (001), (02,11), (13,20), and (060) reflections of the synthetic products, respectively (Vogels et al. 2005b). The *d* value of (006) reflection at 0.153 nm is an indicative evidence for trioctahedral clay minerals. There were no obvious reflections of impurities, indicating that pure saponites have been successfully synthesized. However, the broad and weak (00*l*) reflections suggest that the crystallinity of the synthetic saponites is relatively poor when compared with natural ones.

XRD patterns (Fig. 1) show that relatively strong (001) reflections were recorded in SAP-I-7.89, SAP-I-5.43, and SAP-I-4.50 in Series I, and SAP-II-7.89 and SAP-II-5.43 in Series II, indicating that well-crystallized and ordered saponites were synthesized. With an increase or decrease of Si/Al ratio, the (001) reflection was obviously weakened and broadened, corresponding to poorly crystallized synthetic saponites. However, considering the added amount of Mg in Series II is significantly more than that in the corresponding sample in Series I (Table 1), we can conclude that the initial Si/Al ratio has a more prominent effect on the crystallinity of the synthetic saponites than Mg does.

This is also evidenced by SEM and TEM observations as shown in Figure 2. In the SEM images of SAP-I-5.43 (Fig. 2b) and SAP-I-7.89 (Fig. 2c), well-crystallized layers of saponites can be extensively observed. However, SAP-I-2.33 (Fig. 2a) and SAP-I-39.00 (Fig. 2d) displayed small particle aggregates and some discrete small saponite layers could be observed among particles in SAP-I-39.00. As further indicated by TEM images, the aggregated particles in SAP-I-2.33 (Fig. 2e) contained crystallized small saponite layers with random orientation while SAP-I-5.43 (Fig. 2f) displayed large saponite layers. A small amount of amorphous materials, as determined by selected-area electron diffraction (SAED), were indeed observed in the synthetic saponites. The Si/Al ratios in SAP-I-2.33, SAP-I-5.43, and SAP-I-7.89, derived from energy-dispersive X-ray (EDX) analysis, are ca. 2.4 (average of nine points), 5.9 (average of five points), and 8.1 (average of six points), respectively. These values are comparable to those determined using X-ray fluorescence (XRF) as shown in Table 1.

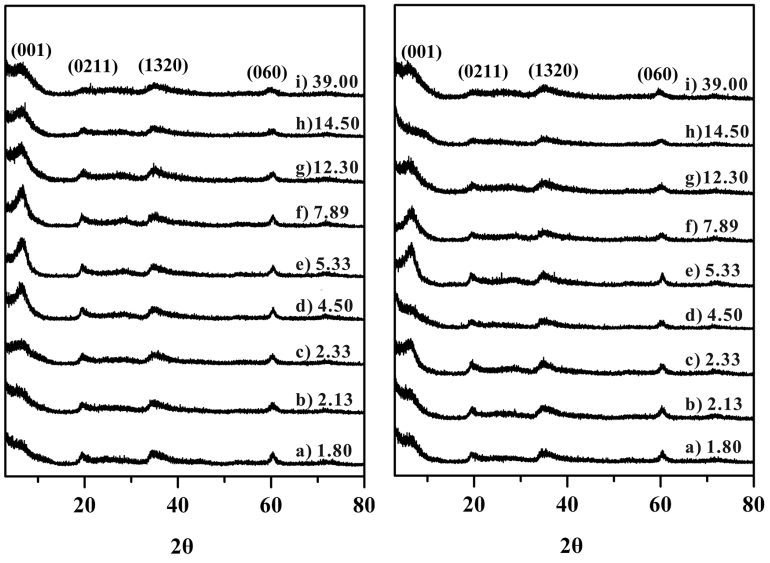

Figure 1. XRD patterns of synthetic saponites in Series I (**left**) with Si/Al molar ratio of (**a**) 1.80, (**b**) 2.13, (**c**) 2.33, (**d**) 4.50, (**e**) 5.43, (**f**) 7.89, (**g**) 12.30, (**h**) 14.50, and (**i**) 39.00, and in Series II (**right**) with Si/Al molar ratio of (**a**) 1.80, (**b**) 2.13, (**c**) 2.33, (**d**) 4.50, (**e**) 5.43, (**f**) 7.89, (**g**) 12.30, (**h**) 14.50, and (**i**) 39.00.

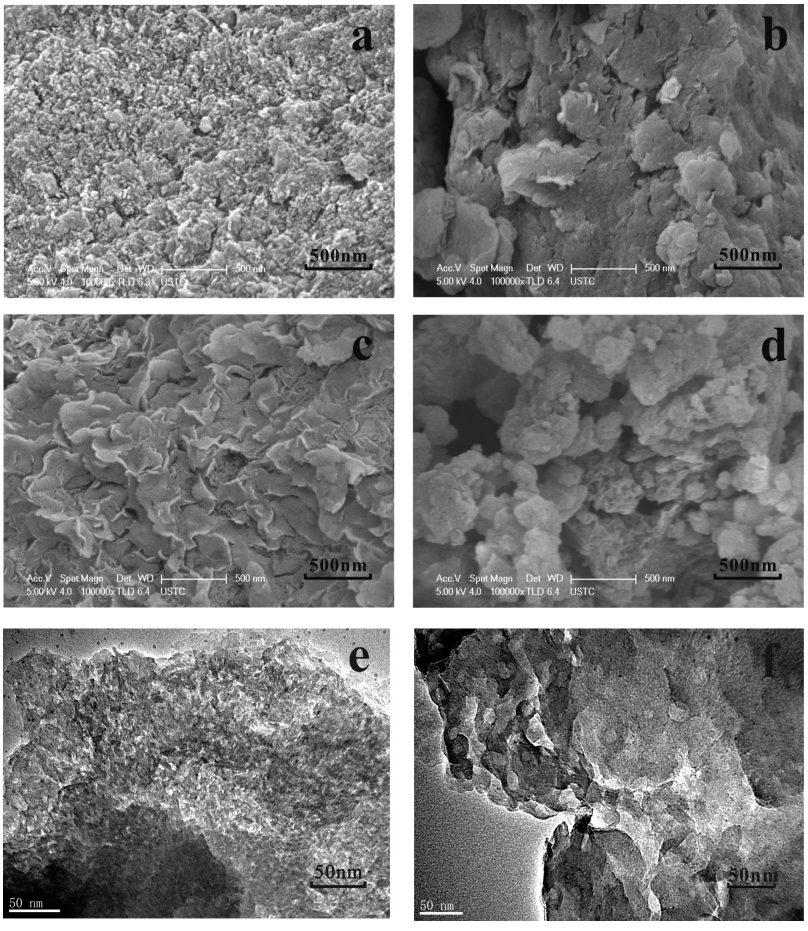

Figure 2. SEM (**a–d**) and TEM (**e–f**) images of synthetic saponites: (**a**) SAP-I-2.33, (**b**) SAP-I-5.43, (**c**) SAP-I-7.89, (**d**) SAP-I-39.00, (**e**) SAP-I-2.33, and (**f**) SAP-I-5.43.

To further identify the successful synthesis of saponites, intercalation experiments with hexadecyltrimethylammonium bromide (HDTMAB) were conducted at a concentration to yield an amount equivalent to the CEC of the saponite and the XRD patterns of the intercalated products are shown in Figure 3. A strong and well ordered (001) reflection with a basal spacing at ca. 2.24 nm for SAP-I-2.33-1CEC (Fig. 3b), 2.83 nm for SAP-I-5.43-1CEC (Fig. 3d), and 2.32 nm for SAP-I-7.89-1CEC (Fig. 3f) were recorded, reflecting a paraffin bilayer arrangement adopted by the intercalated surfactant within the interlayer space. This is similar to HDTMAB modified 2:1 type clay minerals reported in the literature (Lagaly 1981; He et al. 2004). Interestingly, even those poorly crystallized synthetic saponites (e.g., SAP-I-2.33) displayed a (001) reflection with high intensity after intercalation with surfactant. The intercalation experiments clearly showed that layered saponites have been successfully synthesized in this study.

As discussed above, both XRD and electron microscope analysis results showed that saponites have been successfully synthesized and the initial Si/Al ratio is an important factor affecting the order of lamellae stacking and the particle size of the synthetic saponites (Costenaro et al. 2012). This is associated with the distortion extent of the structural units due to the isomorphous substitutions of Al^{3+} for Mg^{2+} in the octahedral sheet and Al^{3+} for Si^{4+} in the tetrahedral sheet.

From Table 1, we can find that the measured Si/Al ratio in the synthetic products of Series II was higher than that in the corresponding samples of Series I, due to a larger added amount of Mg in the starting materials of Series II. As Mg only occupies the octahedral sites in the saponite structure, the difference of the measured Si/Al ratio implies that there is an occupancy competition between Al and Mg, and Mg can readily enter into the octahedral sites prior to Al. This leads to a significant influence on the occupancy of Al ions in octahedral and tetrahedral sites in the saponite structure, which is further supported by MAS NMR spectra (see below).

Occupancy of Al ions in the synthetic saponites

The information about Al occupancy in the synthetic saponites can be obtained from the ^{27}Al MAS NMR spectra (Figs. 4A and 4B). For all samples in the two series, the resonance at approximately 65 ppm, corresponding to Al(IV), is much stronger than that at around 9 ppm, corresponding to Al(VI) (Woessner 1989). This suggests that Al ions prefer to occupy tetrahedral sites instead of octahedral ones.

To investigate the occupancy priority of Al in octahedral and tetrahedral sites, the ratios of Al(IV)/Al(VI) in the synthetic saponites were calculated by deconvolution of ^{27}Al MAS NMR spectra (Table 1). Well-crystallized synthetic saponites (e.g., SAP-I-5.43, SAP-I-7.89, SAP-II-5.43, and SAP-II-7.89) showed a higher Al(IV)/Al(VI) ratio than poorly crystallized synthetic samples and the maximum values were reached in SAP-I-5.43 [Al(IV)/Al(VI) = 25.6] and SAP-II-5.43 [Al(IV)/Al(VI) = 25.3]. It must be noted that all the ^{27}Al MAS NMR spectra of the well-crystallized samples (e.g., SAP-I-5.43, SAP-I-7.89, SAP-II-5.43, and SAP-II-7.89) showed very low intensity of Al(VI) signals while the intensity of Al(IV) signal is comparable to that of the samples with low crystallinity. This suggests that the Al(IV)/Al(VI) ratio has a significant effect on the crystallinity of the synthetic saponite i.e., Al occupancy in octahedral sites has a negative effect on the crystallinity of the synthetic saponites.

The cation exchange capacities (CEC) of the synthetic saponites were determined and shown in Table 1. With the substitutions of Al^{3+} for Si^{4+} and Al^{3+} for Mg^{2+}, the synthetic saponites are negatively charged (Brigatti et al. 2006). It is noteworthy

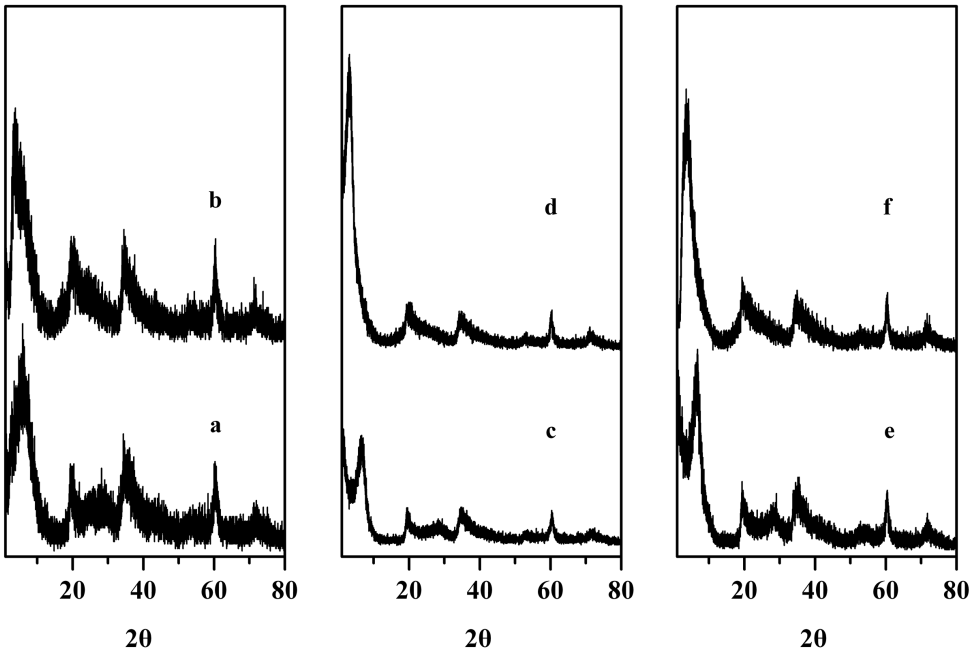

Figure 3. XRD patterns of (**a**) SAP-I-2.33 and (**b**) SAP-I-2.33-1CEC, (**c**) SAP-I-5.43 and (**d**) SAP-I-5.43-1CEC, (**e**) SAP-I-7.89 and (**f**) SAP-I-7.89-1CEC.

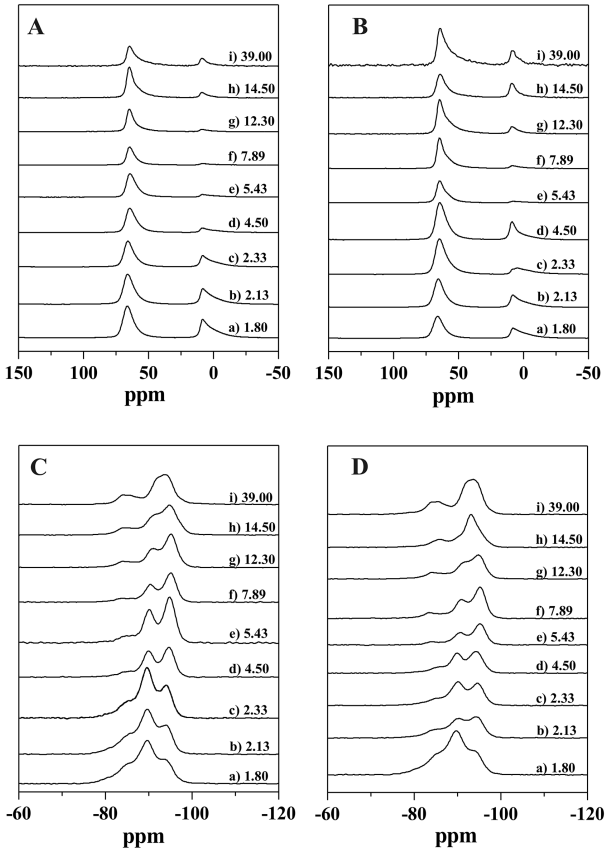

Figure 4. ^{27}Al MAS NMR (**A**–**B**) and ^{29}Si CPMAS NMR (**C**–**D**) spectra of synthetic saponites in Series I (**A**, **C**) with Si/Al molar ratio of (**a**) 1.80, (**b**) 2.13, (**c**) 2.33, (**d**) 4.50, (**e**) 5.43, (**f**) 7.89, (**g**) 12.30, (**h**) 14.50, and (**i**) 39.00, and in Series II (**B**, **D**) with Si/Al molar ratio of (**a**) 1.80, (**b**) 2.13, (**c**) 2.33, (**d**) 4.50, (**e**) 5.43, (**f**) 7.89, (**g**) 12.30, (**h**) 14.50, and (**i**) 39.00.

that those well-crystallized synthetic saponites had a relatively higher CEC value than other samples (Table 1). The substitution of Al^{3+} for Si^{4+} in tetrahedral sheet will result in a negative charge. However, there is two possible ways for substitution of Al^{3+} for Mg^{2+} in the octahedral sheet, i.e., $1Al^{3+} \rightarrow 1Mg^{2+}$ (Suquet et al. 1981) and $2Al^{3+}$ + vacancy $\rightarrow 3Mg^{2+}$ (Vogels et al. 2005b). The case of $1Al^{3+} \rightarrow 1Mg^{2+}$ will result in a positive charge in the synthetic product whereas $2Al^{3+}$ + vacancy $\rightarrow 3Mg^{2+}$ will not lead to any net charge. From Table 1, we can find that the substituting Al^{3+} amount in the tetrahedral sheets decreased with the increment of Si/Al ratio. This means that the CEC of the synthetic saponites should also decrease with the increment of Si/Al ratio if substitution of Al^{3+} for Mg^{2+} in the octahedral sheet occurred as $2Al^{3+}$ + vacancy $\rightarrow$ $3Mg^{2+}$. But CEC measurements showed that the saponites with both relatively high and low Si/Al ratio, corresponding to poorly crystallized samples, had low CEC values. This suggests that substitution of $1Al^{3+} \rightarrow 1Mg^{2+}$ in the octahedral sheets occurred in the saponite synthesis (Bisio et al. 2008).

On the other hand, ^{29}Si CPMAS NMR spectra also provided complementary evidences for Al occupancy (Figs. 4C and 4D). For the well-crystallized synthetic saponites, two well-resolved ^{29}Si signals were recorded at approximately –95 and –91 ppm, corresponding to Q^3 Si(0Al) and Q^3 Si(1Al) [Q^m(nAl)], Q^m (m = 0, 1, 2, 3, 4) refers to the polymerization state of Si, and nAl (n ≤ m) to the number of Al in the next-nearest neighbor tetrahedral position], respectively (Lipsicas et al. 1984). With an increase or decrease of Si/Al ratio, the Q^3 Si(0Al) and Q^3 Si(1Al) signals merged into one broad signal, reflecting a decrease of local structural ordering around Si atoms and crystallinity of the synthetic saponites. This is in agreement with XRD and electron microscope analysis results.

As shown by the ^{29}Si CPMAS NMR spectra, the synthetic saponites with high Si/Al ratio (e.g., SAP-I-39.00) displayed two well-resolved broad signals centered at ca. –94 and –85 ppm, respectively. The broad and asymmetric signal centered at ca. –94 ppm is an overlap of Q^3 Si(0Al) signal at ca. –94 ppm and Q^3 Si(1Al) at ca. –91 ppm as indicated by spectral deconvolution (Fig. 5). With a decrease of Si/Al ratio, a prominent shoulder at ca. –91 ppm corresponding to Q^3 Si(1Al) occurred in the less negative side of the main signal of Q^3 Si(0Al) centered at ca. –95 ppm. The two signals reached a best resolution in SAP-I-5.43, SAP-I-7.89, SAP-II-5.43, and SAP-II-7.89, which are well crystallized as indicated by XRD and SEM observation. When the Si/Al ratio was further decreased, the resolution between Q^3 Si(0Al) and Q^3 Si(1Al) signals decreased and the Q^3 Si(1Al) signal became more prominent than Q^3 Si(0Al). This can be well explained by the change of chemical composition in the synthetic saponites. A decrease of Si/Al ratio reflects more Al ions were incorporated into the saponite structure, resulting in an increase of the Q^3 Si(1Al) signal intensity.

In the ^{29}Si CPMAS NMR spectra of all samples, a signal at –84 to –86 ppm was recorded, which was attributed to Q^3 Si(2Al) in the previous studies (Lipsicas et al. 1984; Delevoye et al. 2003). Interestingly, this signal has never been reported for natural clay minerals. Theoretically, the Q^3 Si(2Al) signal only occurs when the Si/Al ratio in the tetrahedral sheet is less than 3:1. Hence, the relatively high intensity of the resonance around –86 ppm in the synthetic saponites with high Si/Al ratio (e.g., SAP-I-39.00 and SAP-I-14.50) is unlikely attributed to Q^3 Si(2Al) taking into account the low amount of Al^{3+} and the very weak Q^3 Si(lAl) resonance. A most possible attribution of the signal at ca. –86 ppm is to the Q^2 Si(OAl) present at the layer edges of clay minerals (Vogels et al. 2005b).

To elucidate the origin of the signal at ca. –86 ppm, the synthetic saponites were grafted with APTES in a mixture of ethanol-water (75/25, v/v). The obtained ^{29}Si CPMAS NMR spectra of the saponites and grafting products were shown in Figure 5. The occurrence of T^3 and T^2 signals at ca. –67.2 and –57.7 ppm indicated a successful loading of APTES on the saponites and condensation among APTES molecules. After grafting saponites with silane, we can find that the intensity of the signal at ca. –86 ppm decreased whereas those of Q^3 Si(0Al) and Q^3 Si(1Al) increased. If the signal at ca. –86 ppm corresponds to Q^3 Si(2Al), its intensity should not be decreased after the grafting reaction. Hence, the decreased intensity of the signal at –86 ppm and increased intensity of Q^3 Si(0Al) and Q^3 Si(1Al) signals strongly suggest that the Q^2 Si was transformed to Q^3 Si when silane was chemically bonded with the Si atoms at the layer edges (Herrera et al. 2004; Daniel et al. 2008). This indicates

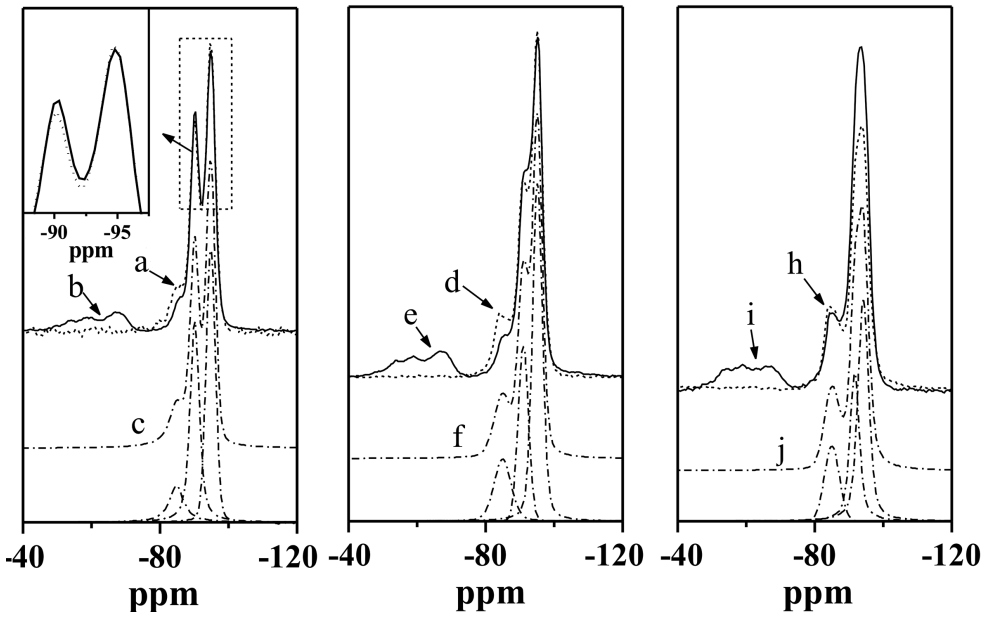

Figure 5. ^{29}Si CPMAS NMR spectra of (**a**) SAP-I-5.43 (dash line) and (**b**) SAP-I-5.43-APTES (solid line), (**c**) deconvoluted spectrum of SAP-I-5.43 (dash dot line) (**d**) SAP-I-12.30 (dash line), (**e**) SAP-I-12.30-APTES (solid line), (**f**) deconvoluted spectrum of SAP-I-12.30 (dash dot line), (**g**) SAP-I-39.00 (dash line), (**h**) SAP-I-39.00-APTES (solid line), and (**i**) deconvoluted spectrum of SAP-I-39.00 (dash dot line).

that the signal at ca. –86 ppm should be attributed to Q^2 Si at the clay layer edges. As shown by TEM and SEM observations, the synthetic saponites are composed of small layers/particles with a high aspect ratio. In this case, the amount of Si atoms situated at the layer edges is relatively large and could be detected by MAS NMR (Daniel et al. 2008). The general absence of the Q^2 Si resonance in the ^{29}Si CPMAS NMR spectra of phyllosilicates may be ascribed to the large particle size of naturally occurring samples (Vogels et at. 2005b).

In addition, we found that the intensity increase of Q^3 Si(0Al) and Q^3 Si(1Al) signals in SAP-I-12.30-APTES and SAP-I-39.00-APTES was more prominent than that in SAP-I-5.43-APTES. Only a slight intensity increase could be seen for SAP-I-5.43-APTES attributed to the effect of particle size. As shown by SEM and TEM images, SAP-I-5.43 displayed larger saponite layers when compared with SAP-I-12.30 and SAP-I-39.00. The higher aspect ratio of saponite in SAP-I-5.43 is a disadvantage for successful silane grafting.

Acknowledgments

This is contribution No. IS-1761 from GIGCAS. The authors thank Brian L. Phillips, J. Theo Kloprogge, and the other two anonymous reviewers for the helpful comments and reviews. This work was financially supported by National Natural Science Foundation of China (Grant No. 41372048) and National Key Technology R&D Program (Grant No. 2011BAB03B06).

References cited

Alexandre, M., and Dubois, P. (2000) Polymer-layered silicate nanocomposites: preparation, properties and uses of a new class of materials. Materials Science and Engineering: R: Reports, 28, 1–63.

Bisio, C., Gatti, G., Boccaleri, E., Marchese, L., Superti, G.B., Pastore, H.O., and Thommes, M. (2008) Understanding physico-chemical properties of saponite synthetic clays. Microporous and Mesoporous Materials, 107, 90–101.

Brigatti, M.F., Galan, E., and Theng, B.K.G. (2006) Structures and mineralogy of clay minerals, In F. Bergaya, B.K.G. Theng, and G. Lagaly, Eds., Handbook of Clay Science, p. 19–86. Elsevier, Amsterdam.

Casagrande, M., Storaro, L., Lenarda, M., and Rossini, S. (2005) Solid acid catalysts from clays: Oligomerization of 1-pentene on Al-pillared smectites. Catalysis Communications, 6, 568–572.

Costenaro, D., Gatti, G., Carniato, F., Paul, G., Bisio, C., and Marchese, L. (2012) The effect of synthesis gel dilution on the physico-chemical properties of acid saponite clays. Microporous and Mesoporous Materials, 162, 159–167.

Daniel, L.M., Frost, R.L., and Zhu, H.Y. (2008) Edge-modification of laponite with dimethyl-octylmethoxysilane. Journal of Colloid and Interface Science, 321, 302–309.

Delevoye, L., Robert, J.-L., and Grandjean, J. (2003) ^{23}Na 2D 3QMAS NMR and ^{29}Si, ^{27}Al MAS NMR investigation of laponite and synthetic saponites of variable interlayer charge. Clay Minerals, 38, 63–69.

Farmer, V.C., Krishnamurti, G.S.R., and Huang, P.M. (1991) Synthetic allophane and layer-silicate formation in SiO_2-Al_2O_3-FeO-Fe_2O_3-MgO-H_2O systems at 23 °C and 89 °C in a calcareous environment. Clays and Clay Minerals, 39, 561–570.

Farmer, V.C., Mchardy, W.J., Elsass, F., and Robert, M. (1994) hk-ordering in aluminous nontronite and saponite synthesized near 90 °C: effects of synthesis conditions on nontronite composition and ordering. Clays and Clay Minerals, 42, 180–186.

Giannelis, E.P., Krishnamoorti, R., and Manias, E. (1999) Polymer-silicate nanocomposites: Model systems for confined polymers and polymer brushes. Advances in Polymer Science, 138, 107–147.

Goto, A., and Tatsumi, Y. (1994) Quantitative analysis of rock samples by an X-ray fluorescence spectrometer (I). The Rigaku Journal, 11, 40–59.

He, H.P., Frost, R.L., Deng, F., Zhu, J.X., Wen, X.Y., and Yuan, P. (2004) Conformation of surfactant molecules in the interlayer of montmorillonite studied by C-13 MAS NMR. Clays and Clay Minerals, 52, 350–356.

He, H.P., Duchet, J., Galy, J., and Gerard, J.F. (2005) Grafting of swelling clay materials with 3-aminopropyltriethoxysilane. Journal of Colloid and Interface Science, 288, 171–176.

He, H.P., Ma, Y.H., Zhu, J.X., Yuan, P., and Qing, Y.H. (2010) Organoclays prepared from montmorillonites with different cation exchange capacity and surfactant configuration. Applied Clay Science, 48, 67–72.

Herrera, N.N., Letoffe, J.M., Putaux, J.L., David, L., and Bourgeat-Lami, E. (2004) Aqueous dispersions of silane-functionalized laponite clay platelets. A first step toward the elaboration of water-based polymer/clay nanocomposites. Langmuir, 20, 1564–1571.

Higashi, S., Miki, H., and Komarneni, S. (2007) Mn-smectites: Hydrothermal synthesis and characterization. Applied Clay Science, 38, 104–112.

Hu, X., Lu, G., and Yang, Y. (2000) Determination of cation exchange capacity in clay $[Co(NH_3)_6]^{3+}$ exchange method. Chinese Journal of Analytical Chemistry, 28, 1402–1405.

Kawi, S., and Yao, Y.Z. (1999) Saponite catalysts with systematically varied Mg/Ni

ratio: synthesis, characterization, and catalysis. Microporous and Mesoporous Materials, 33, 49–59.
Kloprogge, J.T., Breukelaar, J., Jansen, J.B.H., and Geus, J.W. (1993) Development of ammonium-saponites from gels with variable ammonium concentration and water content at low-temperatures. Clays and Clay Minerals, 41, 103–110.
Kloprogge, J.T., Breukelaar, J., Geus, J.W., and Jansen, J.B.H. (1994a) Characterization of Mg-saponites synthesized from gels containing amounts of Na^+, K^+, Rb^+, Ca^{2+}, Ba^{2+}, or Ce^{4+} equivalent to the CEC of the saponite. Clays and Clay Minerals, 42, 18–22.
Kloprogge, J.T., Breukelaar, J., Wilson, A.E., Geus, J.W., and Jansen, J.B.H. (1994b) Solid-state nuclear magnetic resonanse spectroscopy on synthetic ammonium/aluminum-saponites. Clays and Clay Minerals, 42, 416–420.
Kloprogge, J.T., Hickey, L., and Frost, R.L. (1999) Infrared study of some synthetic saponites: Effect of NH_4/Al and H_2O/(Si+Al) ratios during the crystallization. Journal of Materials Science Letters, 18, 1401–1403.
Lagaly, G. (1981) Characterization of clays by organic compounds. Clay Minerals, 16, 1–21.
Lipsicas, M., Raythatha, R.H., Pinnavaia, T.J., Johnson, I.D., Giese, R.F., Costanzo, P.M., and Robert, J.L. (1984) Silicon and aluminium site distributions in 2:1 layered silicate clays. Nature, 309, 604–607.
Mackenzie, R.C. (1957) Saponite from Allt Ribhein, Fiskavaig Bay, Skye. Mineralogical Magazine, 31, 672–680.
Moronta, A. (2004) Catalytic and adsorption properties of modified clay surfaces. Interface Science and Technology, 1, 321–344.
Suquet, H., Malard, C., Copin, E., and Pezerat, H. (1981) Variation du parametre b et de la distance basale d_{001} dans une serie de saponites a charge croissante: I. Etats hydrates. Clay Minerals, 16, 53–67.
Utracki, L.A., Sepehr, M., and Boccaleri, E. (2007) Synthetic, layered nanoparticles for polymeric nanocomposites (PNCs). Polymers for Advanced Technologies, 18, 1–37.
Varma, R.S. (2002) Clay and clay-supported reagents in organic synthesis. Tetrahedron, 58, 1235–1255.
Vicente, I., Salagre, P., Cesteros, Y., Medina, F., and Sueiras, J.E. (2010) Microwave-assisted synthesis of saponite. Applied Clay Science, 48, 26–31.
Vicente Rodriguez, M.A., Suarez Barrios, M., Lopez Gonzalez, J.D., and Banares Munoz, M.A. (1994) Acid activation of a ferrous saponite (griffithite); physicochemical characterization and surface area of the products obtained. Clays and Clay Minerals, 42, 724–730.
Vogels, R.J.M.J., Breukelaar, J., Kloprogge, J.T., Jansen, J.B.H., and Geus, J.W. (1997) Hydrothermal crystallization of ammonium-saponite at 200 °C and autogeneous water pressure. Clays and Clay Minerals, 45, 1–7.
Vogels, R.J.M.J., Kloprogge, J.T., and Geus, J.W. (2005a) Catalytic activity of synthetic saponite clays: effects of tetrahedral and octahedral composition. Journal of Catalysis, 231, 443–452.
——— (2005b) Synthesis and characterization of saponite clays. American Mineralogist, 90, 931–944.
Woessner, D.E. (1989) Characterization of clay minerals by ^{27}Al nuclear magnetic resonance spectroscopy. American Mineralogist, 74, 203–215.
Xue, S., and Pinnavaia, T.J. (2010) Methylene-functionalized saponite: A new type of organoclay with CH_2 groups substituting for bridging oxygen centers in the tetrahedral sheet. Applied Clay Science, 48, 60–66.
Yao, M., Liu, Z.Y., Wang, K.X., Zhu, M.Q., and Sun, H.J. (2005) Application of FTIR technique in microwave-hydrothermal synthesis of saponite. Spectroscopy and Spectral Analysis, 25, 870–873.
Zanetti, M., Lomakin, S., and Camino, G. (2000) Polymer layered silicate nanocomposites. Macromolecular Materials and Engineering, 279, 1–9.
Zhang, D., Zhou, C.H., Lin, C.X., Tong, D.S., and Yu, W.H. (2010) Synthesis of clay minerals. Applied Clay Science, 50, 1–11.

Manuscript received March 20, 2013
Manuscript accepted August 19, 2013
Manuscript handled by Brian Phillips